

QPET: A Versatile and Portable Quantity-of-Interest-preservation Framework for Error-Bounded Lossy Compression

Jinyang Liu
University of Houston
Houston, TX, USA
jliu107@uh.edu

Pu Jiao*
University of Kentucky
Lexington, KY, USA
pujiao@uky.edu

Kai Zhao
Florida State University
Tallahassee, FL, USA
kzhao@cs.fsu.edu

Xin Liang†
University of Kentucky
Lexington, KY, USA
xliang@uky.edu

Sheng Di
Argonne National Laboratory
Lemont, IL, USA
sdi1@anl.gov

Franck Cappello
Argonne National Laboratory
Lemont, IL, USA
cappello@mcs.anl.gov

ABSTRACT

Error-bounded lossy compression has been widely adopted in many scientific domains because it can address the challenges in storing, transferring, and analyzing the unprecedented amount of scientific data. Although error-bounded lossy compression offers general data distortion control by enforcing strict error bounds on raw data, they may fail to meet the quality requirements on the results of downstream analysis derived from raw data, a.k.a Quantities of Interest (QoIs). This may lead to uncertainties and even misinterpretations in scientific discoveries, significantly limiting the use of lossy compression in practice. In this paper, we propose QPET, a novel, versatile, and portable framework for QoI-preserving error-bounded lossy compression, which overcomes the challenges of modeling diverse QoIs by leveraging numerical strategies. QPET features (1) high portability to multiple existing lossy compressors, (2) versatile preservation to most differentiable univariate and multivariate QoIs, and (3) significant compression improvements in QoI-preservation tasks. Experiments with six real-world datasets demonstrate that QPET outperformed existing QoI-preserving compression framework in terms of speed, and integrating QPET into state-of-the-art error-bounded lossy compressors can gain up to 250% compression ratio improvements to original compressors and up to 75% compression ratio improvements to existing QoI-integrated scientific compressors. Under the same level of peak signal-to-noise ratios in the QoIs, QPET can improve the compression ratio by up to 102%.

PVLDB Artifact Availability:

The source code, data, and/or other artifacts have been made available at <https://github.com/JLiu-1/QPET-Artifact>.

1 INTRODUCTION

Today's high-performance computing facilities and high-resolution instruments are producing vast amounts of scientific data that overwhelm the data storage and transmission systems. According to recent studies, climate simulations generate hundreds of TB of data every 16 seconds [13], and fusion applications may produce 1 EB of data in a single run with current- and next-generation exascale computing systems [3]. This poses grand challenges in the underlying data management tasks, including I/O and data transfer, which necessitates the need for effective data compression.

Data compression has been widely used in reducing data volumes [18, 37, 40, 49] and accelerating queries [7, 9, 53, 54] in database and data management systems. Nonetheless, challenges arise when applying existing compression techniques in the context of scientific data. On the one hand, while lossless compression techniques [1, 6, 10, 31, 37] can recover data to the exact precision, they suffer from limited compression ratios in floating-point scientific data and thus fail to meet the desired reduction level in data size. On the other hand, lossy compressors for natural vision data and time-series databases, such as JPEGs [43, 48], H.26x series [8, 40, 49], SummaryStore [4], and ModelarDB [18, 20], cannot provide a quantifiable bound on the errors in the decompressed data, leading to uncertainties in the downstream data visualization and analytics. Under these circumstances, error-bounded lossy compression has been proposed as a viable way to reduce the size of scientific data while providing guaranteed error control.

Over the past years, several error-bounded lossy compressors [24, 27, 29, 30, 35, 44, 45] have been developed and adopted to accelerate data management and analytics in multiple scientific domains. These compressors usually feature strict error control in the decompressed data based on user requirements, such that domain scientists can control the impact of lossy compression according to their specific needs. However, most of the compressors only provide error bounds on the raw data despite the fact that the scientists care more about the errors in their derived quantities or downstream analyses. Such derived information, also known as Quantities of Interest (QoIs), is of utmost importance to the fidelity and integrity of scientific discoveries. Typical QoIs include symbolic functions [19], derivatives and gradients [39], integrals [14], and topological features [26, 51, 52]. Failure to quantify the distortions in QoIs during lossy compression may lead to misinterpretation of the data and even falsified discoveries, significantly limiting the use of error-bounded lossy compressors in practice.

A few QoI-preserving compressors have already been proposed and applied in scientific applications to bridge the gap. For instance, MGARD [5] has enabled the support for bounded linear QoIs, which is further integrated into fusion applications to preserve important derived quantities such as density [15]; variations of SZ have been proposed to tackle the preservation of symbolic QoIs [19], contour tree [52], and critical points in vector fields [26, 51]. Despite those efforts, several significant challenges remain unaddressed in

*Co-first author

†Corresponding author

the context of QoI reservation. (1) Existing QoI-preserving lossy compressors are fine-crafted analytical solutions for particular QoIs, which lose generalization and extensibility to more diverse QoI formats. (2) Most existing methods rely on custom point-wise error bounds to enable the preservation of QoIs, but effectively determining or storing these error bounds is non-trivial. (3) Existing approaches usually tightly couple the QoI-preserving mechanism and compression pipeline, which prohibits the use of more advanced or newly developed compression methods and limits the efficiency.

To address those challenges, we propose QPET, a novel, versatile, and portable framework based on error-bound auto-tuning to tackle the efficient preservation of symbolic QoIs. In particular, we notice that various symbolic QoIs can be modeled in mathematical formats composed of differentiable functions. Moreover, the numerical approximations of the QoIs with simplified format (e.g., Taylor expansion with second-order derivatives) can provide a unified, efficient, and well-performing algorithmic routine to determine the point-wise error bounds. Thus, we can develop a QoI-preserving framework, which can easily adapt to diverse QoIs and the compression pipelines adopted by lossy compressors in a highly optimized scheme. In summary, our contributions are three-fold:

- We propose QPET, a QoI-oriented Point-wise Error-bound auto-Tuning framework to enable the preservation of diverse QoIs in scientific applications. In particular, QPET leverages numerical and probabilistic methods to derive sufficient error bounds on each data point, which easily adapts to most differentiable QoIs.
- QPET effectively determines the best-fit point-wise error bound for each data value in the QoI-preserving compression. It also jointly optimizes the error-bound storage overhead and the reduction in raw data by a dynamic global error bound selection.
- We integrate QPET into 3 state-of-the-art error-bounded lossy compressors and evaluate them with solid benchmarks. Experimental results demonstrate that QPET-integrated compressors yield significant compression ratio (CR) and QoI quality gains in QoI-preserving compression tasks. Under the same QoI error threshold, QPET-integrated compressors achieve up to 250% CR improvements over the base compressors and up to 75% CR improvements over existing QoI-preserving lossy compressors. Under the same peak signal-to-noise ratios (PSNR) in QoIs derived from the decompressed data, the CR can also be increased by up to 102% compared to the baselines.

We organize the rest of this paper as follows: Section 2 discusses the related work of this paper. In Section 3, we formulate and clarify our research motivation and target. In Section 4, we propose the high-level design of QPET, specifying its components, overall algorithm, and integration. Section 5 demonstrates the detailed designs and algorithms in QPET. In Section 6, we present the evaluations of QPET. Section 7 concludes this work and discusses future plans.

2 RELATED WORK

This section discusses the related work of this paper in three aspects, covering traditional compression techniques used in database systems, emerging lossy compressors for scientific data, and state-of-the-art QoI-preserving lossy compression methods.

Traditional compression techniques for database systems: Various data compressors have been proposed for large-scale databases

in diverse data domains and formats. Generic lossless compressors such as GZIP [11], ZSTD [10], and LZ4 [36] are widely used to compress various types of data to reduce storage requirement [18, 37, 40, 49] and accelerating queries [7, 9, 53, 54]. With the increasing amount of floating-point data in applications, several compressors have been proposed to specifically deal with floating-point data. A typical example is ndZip [21, 22], which leverages Lorenzo prediction [17] and residual encoding to compress floating-point data with high efficiency. To handle different types of data, Gorilla [37] and Chimp [25] have been designed for time-series data, and Buff [32] has been tailored to process low-precision data. Despite their ability to recover the exact data, lossless compressors usually exhibit low compression ratios, which severely limits their use in practice.

To address the limited compression ratios in lossless compressors, lossy compression has been proposed as an alternative way to reduce data in database systems. Regarding lossy database compression methods, iModelarDB [18, 20] summaryStore [4] are designed for time-series data, which leverage data-processing techniques including PMC-mean [23] and the linear Swing model [12].

Emerging lossy compression techniques for scientific data: To process the high volumes of scientific data while ensuring the quality of decompressed data for accurate post hoc analytics, scientific data compressors require not only decent compression ratios but also strict error control, where error-bounded lossy compression is becoming a promising option. Error-bounded lossy compressors allow users to specify an error bound as a compression parameter, and ensure the element-wise difference between the original data and decompressed data is less than the error bound.

SZ3 [29, 55] is one of the most widely used error-bounded lossy compressors with a prediction-based design. It utilizes dynamic spline functions to approximate the data, followed by a linear-scaling quantization method [41] and lossless encoding methods to achieve size reduction with guaranteed error control. Later, HPEZ [35] is proposed to significantly improve the quality of SZ3 via more complex interpolation schemes and quality-oriented auto-tuning mechanisms. Another category of error-bounded lossy compressors relies on domain transform for decorrelation. For instance, ZFP [30] is a fast and highly parallel compressor using near-orthogonal block transform, and SPERR [24] utilizes more complex wavelet transforms to obtain better compression quality at the cost of lower compression throughput. While error-bounded lossy compressors have guaranteed error control on the decompressed data, they cannot provide a quantifiable error bound on the downstream QoIs, as the QoIs could be highly diverse and non-linear.

QoI-preserving lossy compression methods: Variations of error-bounded lossy compressors have been proposed to enable error control for various QoIs. MGARD [5] is one of the first compressors to enable QoI preservation, but it can only provide guaranteed error control for bounded-linear QoIs. In [28], cpSZ has been proposed to preserve the locations and types of critical points in piece-wise linear vector fields. In particular, it carefully derived sufficient point-wise error bounds based on the target QoI, and leveraged it to guide the compression procedure for effective QoI preservation. This idea is further extended to cover the preservation of critical points in multilinear vector fields [26], critical points extracted by sign-of-determinant predicates [51], contour trees [52], and symbolic QoIs [19].

Despite the rapid development of QoI-preserving lossy compressors, most existing methods suffer from low generalizability and adaptability. In particular, these compressors have to design specific error control mechanisms toward the target QoI, which is hard to generalize to new sets of QoIs. In addition, most existing works are tightly coupled to a specific compression pipeline, making it difficult to integrate with newly developed compression methods. In this work, we propose a portable module that can easily adapt to diverse QoIs and compression methods. This will significantly improve the efficiency and usability of QoI-preserving lossy compression.

3 BACKGROUND

In this section, we introduce the background for the proposed work. In particular, we define the target QoIs to preserve, followed by a formulation of the QoI-preserving lossy compression problem.

3.1 Quantities of Interest in Scientific Data

As discussed in the previous sections, scientific applications usually require the preservation of QoIs to ensure the integrity of scientific discoveries if lossy compression is used. QoIs represent any derived information that is computed from the raw data, including physical properties [15], derivatives [39], and topological features [52].

In this work, we mainly target the preservation of symbolic QoIs as defined in previous work [19], which can be formulated as univariate and multivariate functions of the input data. This covers a wide range of QoIs in scientific applications, including kinetic energy in cosmology, density in fusion energy science, and vector magnitude in climatology. While four families of QoIs (polynomials, logarithmic mapping, weighted sums, and isosurfaces) can be preserved by prior work [19], the method cannot be generalized to other QoIs easily because it heavily relies on the analytical form of the QoIs to derive the point-wise error bounds on raw data. In this work, we aim to deal with QoIs using numerical strategies, which allow for the same interfaces for diverse sets of QoIs. By approximating QoIs with the second-order Taylor expansion, the proposed framework is much more inclusive than the existing works. Specifically, our framework can support any QoIs that can be expressed by a well-conditioned mathematical function. This will significantly expand the functionality of QoI-preserving lossy compressors to facilitate their use in diverse scientific applications.

In the following, we list the set of target QoIs that can be preserved by the proposed framework. They can be broadly categorized into univariate QoIs and multivariate QoIs, as defined below.

Univariate QoIs: Any second-order differentiable QoI functions, particularly the elementary functions, which are the combination of the following basic functions:

- Polynomial functions such as x^2 , x^3 , and $x^2 + x + 1$;
- Exponential functions such as 2^x and e^x ;
- Logarithm functions such as $\log x$ and $\ln x$;
- Generalize power functions such as $(x + c)^{-1}$ (i.e., $\frac{1}{x+c}$);

Composite elementary functions such as Sigmoid $\sigma(x) = \frac{1}{1+e^{-x}}$ and Hyperbolic Tangent $\tanh x = \frac{e^x - e^{-x}}{e^x + e^{-x}}$ can also be supported.

Multivariate QoIs: Any differentiable multivariate functions in the format of $F(x_1, x_2, \dots, x_n)$, in which $\{x_1, x_2, \dots, x_n\}$ are a set of data points, are also supported by QPET. The point set can be a

data region or the scalar components of a vector data entry. Typical examples include:

- Regional sum/average of univariate QoI ($\frac{1}{n} \sum x^2$);
- velocity scalar of 3-D velocity vector ($\sqrt{v_x^2 + v_y^2 + v_z^2}$);
- Kinetic energy of 3-D velocity vector ($\frac{1}{2}m(v_x^2 + v_y^2 + v_z^2)$);
- Multiplications of scalars (xyz);

Last, the inclusivity of our framework also enables it to preserve **isolines** (data value thresholds) [19] and **piece-wise QoIs** composed by the functions mentioned above. The theoretical foundations and algorithmic implementations of preserving those QoIs will be demonstrated in Section 5.

3.2 QoI-preserving Lossy Compression

Similar to existing works [19], we define QoI-preserving lossy compression as lossy compression algorithms that provide guaranteed error control in both the downstream QoIs and the raw data. The mathematical formulation is as follows.

Suppose we have an input data $X = \{x_i\}$, and a pair of Compressor and Decompressor (Cmp, Dec) that process X to compressed data $C = \text{Cmp}(X)$ and decompressed data $D = \{d_i\} = \text{Dec}(C)$. Given a QoI function Q (which maps data X to another set of data values $Q(X)$), a data error bound ϵ , and a QoI error threshold τ , in QoI-preserving error-bounded lossy compression, we require the errors of data and QoI are both bounded (Eq. 1):

$$C = \text{Cmp}(X), D = \text{Dec}(C) \\ \text{s.t. } \|X - D\|_\infty \leq \epsilon \text{ and } \|Q(X) - Q(D)\|_\infty \leq \tau \quad (1)$$

Our research would like to optimize Cmp and Dec to maximize the compression ratio. Because most QoIs are non-linear, setting a uniform error bound on each data point will result in divergent QoI errors. To address this issue, existing approaches [19, 26, 28] apply different point-wise error bounds on each data point to achieve effective QoI preservation. Nonetheless, these methods focused more on the derivation of the error bounds and overlooked their storage overhead, leading to suboptimal overall compression ratios. To optimize this strategy, targeting selecting the best-fit point-wise error bound (composing a set of $\{\epsilon_i\}$) for each data point such that $|x_i - x'_i| \leq \epsilon_i$ to maximize compression ratio, we need to jointly optimize the compressed data size by error bounds $\{\epsilon_i\}$ ($|\text{Cmp}_{\{\epsilon_i\}}(X)|$) and the compressed error-bound size of $\{\epsilon_i\}$ themselves ($|\text{Cmp}(\{\epsilon_i\})|$). This optimization problem is shown in Eq. 2 and will be specified in Section 5.

$$\{\epsilon_i\} = \arg \max_{\{\epsilon_i\}} \frac{|X|}{|\text{Cmp}_{\{\epsilon_i\}}(X)| + |\text{Cmp}(\{\epsilon_i\})|} \\ \text{s.t. } \|X - D\|_\infty \leq \epsilon \text{ and } \|Q(X) - Q(D)\|_\infty \leq \tau \quad (2)$$

4 QPET DESIGN OVERVIEW

In this section, we provide an overview of the proposed QPET (QoI-oriented Point-wise Error-bound Tuning) framework, describe the underlying QoI-preserving error-bounded lossy compression algorithm, and feature its integration into several existing error-bounded lossy compressors.

4.1 QPET composition

In Figure 1, we demonstrate the composition of the QPET framework that provides QoI-preservation functionality, presenting how it integrates and interacts with general modular scientific error-bounded lossy compression pipelines such as SZ [27, 29, 33, 35, 55] and SPERR [24]. Compared to existing QoI-preserving work [19], QPET introduces several brand-new or improved strategies to cover a wide range of QoI constraints and deliver much higher compression ratios. The components of QPET are:

- **QoI Analyzer:** This symbolic module creates interfaces for efficient evaluations of the QoI function and its derivatives. It auto-deduces the QoI derivatives and converts the symbolic QoI functions/derivatives to built-in numerical functions. Currently, the implementation is based on SymEngine [2].
- **Point-wise Error Bound Estimator:** To constrain the QoI error, this module computes an estimated best-fit compression error bound separately for each input data point.
- **Global Error Bound Auto-tuner:** This module auto-tunes the best-fit global data error bound for the compression.
- **Error Bound Compressor:** This module compresses and stores the point-wise error bounds (this is an optional module because some compression pipelines cannot support point-wise error bounds). QPET follows a lossy scheme described in [19, 28].
- **QoI Validator:** This module verifies the QoI constraints during online data prediction-quantization processes and corrects out-of-constraint data points by lossless storage.

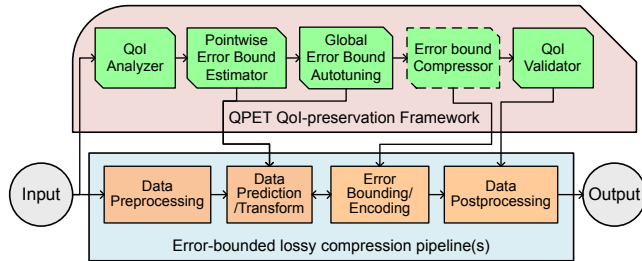


Figure 1: QPET framework and integration

4.2 QPET-integrated Compression Algorithm

Leveraging our proposed QPET framework, Algorithm 1 presents the process of QoI-preserving lossy compression. Some details of this algorithm are explained as follows:

- In Line 1, the QoI Analyzer analyzes input QoI and creates numerical interfaces for QoI/derivatives evaluations.
- In Line 5 and Line 10, the point-wise data error bounds are computed according to QoI types (corresponding to the Point-wise Error Bound Estimator, detailed in Section 5.1 and 5.2).
- In Line 13, from the point-wise error bounds, the global data error bound is auto-tuned by the Global Error Bound Auto-tuner (detailed in Section 5.3).
- In Line 17, the data and point-wise error bounds are compressed.
- In Line 18, the QoI validator module checks the compression QoI errors. The data points that bring out-of-bound QoI errors will be losslessly encoded and appended to the compressed data as corrections to the decompression result.

Algorithm 1 QoI ERROR-CONSTRAINED ERROR-BOUNDED LOSSY COMPRESSION WITH QPET

Input: input data $X = \{x_i\}$ of size n , initial global error bound ϵ , QoI function Q , QoI error threshold t
Output: Compressed data C

```

1: QoIAnalysis( $Q$ ) /*Pre-analysis of QoI constraint*/
2:  $\{\epsilon_i\} \leftarrow \{\epsilon\}$  /*Initialize point-wise error bounds*/
3: if isUnivariate( $Q$ ) then /* $F$  is univariate*/
4:   for  $i = 1 \rightarrow n$  do
5:      $\epsilon_i \leftarrow$  GetPointwiseEB_UniVar( $x_i, Q, t, \epsilon$ ) /*Compute point-wise data error bounds by Algorithm 2*/
6:   end for
7: else /* $Q$  is multivariate*/
8:   for  $i = 1 \rightarrow n_r$  do /* $n_r$  is number of data regions */
9:      $R_i \leftarrow$  GetDataRegion( $i$ )
10:     $E_i \leftarrow$  GetPointwiseEB_MulVar( $R_i, Q, t, \epsilon$ ) /*Compute point-wise data error bounds  $E_i$  for data region  $R_i$  by Algorithm 3*/
11:   end for
12: end if
13:  $\epsilon_g \leftarrow$  TuneGlobalEB( $\{\epsilon_i\}$ ) /*Auto-tune global error bound by Algorithm 4*/
14: for  $i = 1 \rightarrow n$  do
15:    $\epsilon_i \leftarrow \min(\epsilon_i, \epsilon_g)$  /*Update point-wise data errors bound with new global error bound*/
16: end for
17:  $X', C \leftarrow$  Compress( $X, \{\epsilon_i\}, \epsilon_g$ ) /*Compress input data with tuned error bounds.  $C$  and  $X'$  are the compressed data and decompressed data.*/
18:  $X_o \leftarrow$  QoIValidation( $X, X', Q, t$ ) /*Validate QoI errors and collect out-of-constraint data*/
19:  $C \leftarrow C +$  Lossless_Compress( $X_o$ ) /*Losslessly compress  $X_o$  and append the compressed data to  $C$ */
20: return  $C$ 

```

4.3 QPET Integration

Attributed to the high portability and adaptability of HPEZ to existing error-bounded lossy compression pipelines, it can be integrated into a large variety of compressors. In this work, we have integrated QPET into three representative state-of-the-art scientific error-bounded lossy compressors with 2 archetypes: SZ3 [29, 55], HPEZ [35], and SPERR [24]. SZ3 and HPEZ are interpolation-prediction-based compressors, and SPERR is a wavelet-transform-based compressor. According to a recent study [24, 35, 55], those compressors are the top-performing scientific compressors, and their QPET-integrated derivations will also become the top choices of QoI-preserving compression tasks.

5 QOI-PRESERVING ERROR-BOUND COMPUTATION AND OPTIMIZATION

The core of the QPET framework is to provide optimized point-wise and global error bounds for the QoI-preserving lossy compression. In this section, we will feature the algorithms for this task. First, we discuss the univariate QoI cases and then extend it to multivariate QoI functions. Last, we explain how to auto-tune the global data error bound according to the computed point-wise error bounds to optimize the compression ratio. In Table 1, we list the commonly used mathematical notations in the rest of this paper.

5.1 Computing Point-wise Error Bounds with Univariate QoI

We formulate the optimization of the error-bounded lossy compression with point-wise QoI as follows. For each data point x_i in the input data, given a (initial) global error bound ϵ_g , a QoI function f , and a QoI error threshold t , we need to find the optimized point-wise error bound ϵ_i of x_i from the following problem:

Table 1: Notations

Symbol	Description
$X(\{x_i\})$	Input Data(set)
x_i	Input data point
$X'(\{x'_i\})$	Decompressed Data(set)
x'_i	Decompressed data point
ϵ	General data error bound
ϵ_g	Global data error bound
$\epsilon_i(\{\epsilon_i\})$	Pointwise data error bound (set)
Q	General QoI function
f	Univariate QoI function
F	Multivariate QoI function
τ	General QoI error threshold
t	Univariate QoI error threshold
T	Multivariate QoI error threshold

$$\begin{aligned} \epsilon_i &= \max \epsilon \\ \text{s.t. } \epsilon &\leq \epsilon_g, \\ \text{and } |x'_i - x_i| &\leq \epsilon \implies |f(x'_i) - f(x_i)| \leq t \end{aligned} \quad (3)$$

Eq. 3 guarantees that compressing x_i with error bound ϵ_i can both bound the global data and QoI errors with required thresholds. Meanwhile, it is maximized to optimize the data compression ratio. We can optimize this compression task if we can solve ϵ_i effectively from Eq. 3. When the QoI function f has a simple format, such as linear, quadratic, or simply logarithmic, Eq. 3 may also have analytical solutions [19]. However, analytical solutions have limitations: their existence and computational efficiency depend highly on the QoIs. Each analytical solution is customized for a separate QoI, and the computation method cannot be extended to generalized QoIs. To this end, our work proposes a numerical solution that provides a generalized and efficient approximation method for ϵ_i with a wide range of QoI formats. Specifically, as long as f is second-order differentiable (any elementary function is infinitely differentiable), when computing ϵ_i for data point x_i , we will use its second-order Taylor expansion $f_2(x'_i) = f(x_i) + f'(x_i)(x'_i - x_i) + \frac{f''(x_i)}{2}(x'_i - x_i)^2$ to estimate the QoI value at the decompressed data x'_i . In particular, this Taylor expansion with the third-order remainder is:

$$f(x'_i) = f_2(x'_i) + \frac{f'''(\xi)}{3!}(x'_i - x_0)^3, \quad (4)$$

where ξ is a specific value in the interval $[x_i, x'_i]$ (or $[x'_i, x_i]$ if $x'_i < x_i$). Given the error bound ϵ_i which ensures $x'_i \in [x_i - \epsilon_i, x_i + \epsilon_i]$ and assuming $f'''(x)$ is bounded in $[x_i - \epsilon_i, x_i + \epsilon_i]$ by $|f'''(x)| \leq M$, the remainder $\frac{f'''(\xi)}{3!}(x - x_0)^3$ would be smaller than $\frac{M^3}{6}\epsilon_i^3$, i.e. $|f_2(x'_i) - f(x_i)| \leq \frac{M^3}{6}\epsilon_i^3$. With f_2 , we can efficiently compute a good estimation for the best-fit ϵ_i by the following theorem:

THEOREM 5.1. *Given second-order differentiable QoI function f , a global error bound ϵ_g , and a QoI error threshold t , for each data point x_i , if $f''(x_i) \neq 0$, an estimation for the best-fit data error bound ϵ_{x_i} of data point x_0 to fit its QoI error threshold will be $\min\left(\epsilon_g, \frac{\sqrt{|a|^2 + 2|b|t} - |a|}{|b|}\right)$, in which $a = f'(x_i)$ and $b = f''(x_i)$.*

PROOF. Using $f_2(x) = x_0 + a(x - x_0) + \frac{b}{2}(x - x_0)^2$ as an approximation of f , we first find the maximum ϵ so that $|x_1 - x_0| \leq \epsilon \implies |f(x_1) - f(x_0)| \approx |f_2(x_1) - f_2(x_0)| \leq |a(x_1 - x_0) + \frac{b}{2}(x_1 - x_0)^2| \leq t$. This is equivalent to maximizing ϵ which satisfies that $[-\epsilon, \epsilon] \subseteq A$, in which A is the solution set of $|ax + \frac{b}{2}x^2| \leq t$.

By solving $|ax + \frac{b}{2}x^2| \leq t$ (for simplicity we omit the detailed process), we can acquire that $\max \epsilon = \frac{\sqrt{|a|^2 + 2|b|t} - |a|}{|b|}$. Considering the global ϵ_g , finally $\epsilon_{x_0} = \min\left(\epsilon_g, \frac{\sqrt{|a|^2 + 2|b|t} - |a|}{|b|}\right)$. \square

Theorem 5.1 is valid when $b = f''(x_0) \neq 0$. Under $f''(x_0) = 0$, we have the following theorem as a supplement of Theorem 5.1, whose proof is intuitively trivial:

THEOREM 5.2. *Given a second-order differentiable QoI function f , a global error bound ϵ_g , and a QoI error threshold t , for a data point x_0 that $f''(x_0) = 0$, an estimation for the best-fit data error bound of x_0 will be $\min\left(\epsilon_g, \frac{t}{|f'(x_0)|}\right)$ if $f'(x_0) \neq 0$, or ϵ_g when $f'(x_0) = 0$.*

Theorem 5.1 and Theorem 5.2 cover all the cases for best-fit point-wise error-bound estimation. In Figure 2, based on different point-wise QoIs and QoI error tolerances, we plot the point-wise error bounds for different data values from both analytical solutions and our proposed estimation method. Although there are a few inaccurate cases (e.g., $f(x) = x^3$ and close-to-zero data values), our estimation of error bounds achieves very low relative error in most circumstances. It works excellently on estimating low error bounds, critical in preserving the compression ratio and quality in QoI-preserving lossy compression (to be detailed in Section 5.3). The entire process of determining point-wise data error bound with point-wise QoIs is featured in Algorithm 2, which will also be an essential base when dealing with other types of QoI.

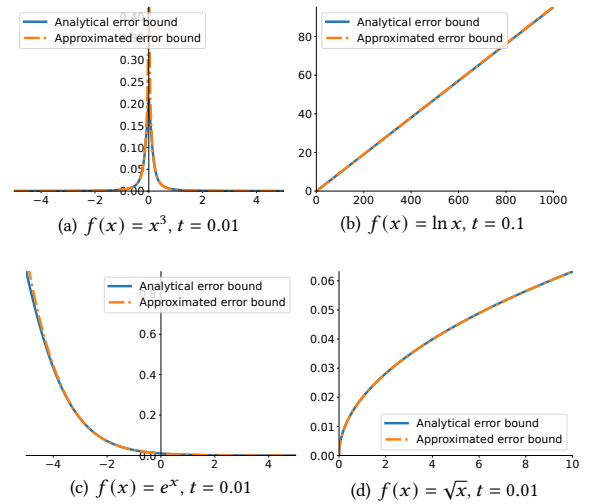


Figure 2: Analytical and estimation point-wise data error bounds of different QoI function $f(x)$ and error threshold t .

Last, we present some necessary clarifications for our method: (1) Besides the derivatives, QPET also collects the information of the singularity point (such as non-defined or non-differentiable points) of f to ensure the computed error bounds fall in the domain of f and convergence range of f_2 . (2) The evaluations of the QoI function and its derivatives are done in native C++ methods, guaranteeing the efficiency of derivative evaluation in Algorithm 2.

Algorithm 2 POINT-WISE ERROR BOUND ESTIMATION WITH UNIVARIATE QoI

Input: input data $X = \{x_i\}$ of size n , global error bound ϵ_g , QoI function f , point-wise QoI error threshold t

Output: Approximated optimized point-wise data error bounds $\{\epsilon_i\}$

```

1:  $d_1(x) \leftarrow f'(x)$  /*Get the efficient process for the first-order derivative*/
2:  $d_2(x) \leftarrow f''(x)$  /*Get the efficient process for the second-order derivative*/
3: for  $i = 1 \rightarrow n$  do
4:    $a \leftarrow d_1(x_i)$ 
5:    $b \leftarrow d_2(x_i)$ 
6:   if  $b \neq 0$  then
7:      $\epsilon_i \leftarrow \frac{\sqrt{|a|^2+2|b|t-|a|}}{|b|}$  /*Compute  $\epsilon_i$  with both derivatives*/
8:   else if  $a \neq 0$  then
9:      $\epsilon_i \leftarrow \frac{t}{|a|}$  /*Compute  $\epsilon_i$  with only first-order derivative*/
10:  else
11:     $\epsilon_i \leftarrow \epsilon_g$  /*set  $\epsilon_i$  as  $\epsilon_g$ */
12:  end if
13:   $\epsilon_i \leftarrow \min(\epsilon_g, \epsilon_i)$ 
14: end for
15: return  $\{\epsilon_i\}$ 

```

5.2 Computing Point-wise Error Bounds with Multivariate QoI

Regarding the error constraining for multivariate QoIs, we actually deal with QoI functions in the format of $F(x_1, \dots, x_n)$. $\{x_i\}$ is a set of data points from the input, and this set can have different forms, such as data blocks, neighbor points, or scalar components of a vector. Given a multivariate QoI $F(x_1, \dots, x_n)$, and a tolerance T for which we requires that $|F(x'_1, \dots, x'_n) - F(x_1, \dots, x_n)| \leq t$ ($\{x'_i\}$ are decompressed values of $\{x_i\}$), we will determine a set of error bounds $\{\epsilon_i\}$ so that

$$\forall i, |x'_i - x_i| \leq \epsilon_i \implies |F(x'_1, \dots, x'_n) - F(x_1, \dots, x_n)| \leq T.$$

In other words, compressing each x_i with error bound ϵ_i will lead the QoI error to be constrained, and we will optimize $\{\epsilon_i\}$ for the best compression ratio. In the next, we will first discuss the theories and algorithm for optimizing $\{\epsilon_i\}$ when $F(x_1, \dots, x_n)$ is the linear combination of univariate QoI functions. Then, we will show how to extend the methodology to generalized cases.

5.2.1 Multivariate QoI in linear format. We first demonstrate our strategy for multivariate QoI functions in the format of

$$F(x_1, \dots, x_n) = C + \sum_i \alpha_i f(x_i) \quad (5)$$

in which C and α_i are constant coefficients, and f can be regarded as a point-wise QoI function. Many common multivariate QoIs [19] are in this format, such as region sum, the (weighted) average of a data block, or the difference-based Laplacian operator [39]. Therefore, it is critical that we present a good solution for this linear format. Suppose we have a set of optimized point-wise tolerances $\{t_i\}$ from the following optimization problem:

$$\begin{aligned} & \text{Optimize } \{t_i\} \\ & \text{s.t. } \forall i, |f(x'_i) - f(x_i)| \leq t_i \\ & \implies |F(x'_1, \dots, x'_n) - F(x_1, \dots, x_n)| \leq T \end{aligned} \quad (6)$$

Then we can optimize the point-wise data error bound $\{\epsilon_i\}$ for set $\{x_i\}$ from those $\{t_i\}$ with Algorithm 2, as in this case we are just bounding point-wise QoI f error within t_i . Therefore, by solving Eq. 6 we can find a way to optimize $\{\epsilon_i\}$. Regarding the optimization target of Eq. 6, intuitively, we can maximize $\sum_i t_i$. However,

this optimization target sometimes leads to skewed distributions of t_i and ϵ_i values over different i . Preliminary works [19] and our experiments showed that point-wise error bounds with skewed distribution would cause the compression ratio to decrease significantly. Therefore, we select to maximize $\min t_i$, equivalent to ensure $t_i = t$ for each i . According to our preliminary experiments, this scheme is better than other intuitive strategies, such as aligning $\alpha_i t_i$. Moreover, if we denote D_i as $f(x'_i) - f(x_i)$, we will notice that $F(x'_1, \dots, x'_n) - F(x_1, \dots, x_n) = \sum_i \alpha_i D_i$. To this end, we can convert Eq. 6 to a more concise format:

$$\begin{aligned} & \text{Optimize } t \\ & \text{s.t. } \forall i, |D_i| \leq t \implies \left| \sum_i \alpha_i D_i \right| \leq T \end{aligned} \quad (7)$$

Next, we will show two solutions of Eq.7, which contribute collaboratively to optimizing t , $\{\epsilon_i\}$, and the compression ratio. First, we have a solution of t that deterministically matches Eq.7:

THEOREM 5.3. *If $t = \frac{T}{\sum_i |\alpha_i|}$, then $|D_i| \leq t \implies |\sum_i \alpha_i D_i| \leq T$.*

PROOF. $|\sum_i \alpha_i D_i| \leq \sum_i |\alpha_i| |D_i| \leq t \sum_i |\alpha_i| = T$. \square

Unfortunately, Theorem 5.3 sometimes presents over-conservative values for t . Fortunately, we have another strategy for determining t . If we regard the $\{D_i\}$ as random variables with the following assumptions: 1) $\{D_i\}$ are independent; 2) D_i has symmetric distribution regarding zero (so $E(D_i) = 0$). Since $|D_i| \leq t$, according to [46, 47], $\{D_i\}$ are sub-Gaussian, and the following concentration inequality holds for each $T > 0$ [16, 46, 47]:

$$P(|\sum_i \alpha_i D_i| \geq T) \leq 2e^{-\frac{T^2}{2\sum_i \alpha_i^2 \sigma_i^2}} \quad (8)$$

σ_i^2 is called the *variance proxy* of D_i . For finite-bounded $|D_i| \leq t$, we have $\sigma_i \leq t$ [46, 47]. QPET uses a single estimation $\sigma_0 = \frac{t}{c}$ for all D_i , in which $c \leq 1$ and σ_0 represents the estimated standard variance of D_i . For example, $c = \sqrt{3}$ and $\sigma_0 = \frac{t}{\sqrt{3}}$ correspond to the uniform distribution over $[-t, t]$. With σ_0 and Eq. 8, we can set up another estimation of an optimized t for Eq. 7:

THEOREM 5.4. *A multivariate QoI function $F(x_1, \dots, x_n) = C + \sum_i \alpha_i f(x_i)$ and the corresponding QoI error threshold T are given. On $\{x_1, \dots, x_n\}$, if the point-wise QoI error D_i is σ_i -Sub-Gaussian in which $\sigma_i \leq \frac{\max D_i}{c}$, for each confidence level of β , taking point-wise QoI error threshold $t = \max |f(x'_i) - f(x_i)| = cT \sqrt{\frac{1}{2\sum_i \alpha_i^2 \ln \frac{2}{1-\beta}}}$, the global QoI error threshold can be guaranteed in a confidence level of β , i.e.: $P(|F(x'_1, \dots, x'_n) - F(x_1, \dots, x_n)| \leq T) \geq \beta$.*

PROOF. Using $\sigma_i = \frac{t}{c}$, for $\{x_1, \dots, x_n\}$, from Eq. 8 we have $P(|F(x'_1, \dots, x'_n) - F(x_1, \dots, x_n)| \geq T) = P(|\sum_i \alpha_i D_i| \geq T) \leq 2e^{-\frac{c^2 T^2}{2t^2 \sum_i \alpha_i^2}} = 2e^{-\ln \frac{2}{1-\beta}} = 1 - \beta$. Therefore, $P(|F(x'_1, \dots, x'_n) - F(x_1, \dots, x_n)| \leq T) = 1 - P(|F(x'_1, \dots, x'_n) - F(x_1, \dots, x_n)| \geq T) \geq \beta$. \square

Because Theorem 5.3 and 5.4 fits in different cases when optimizing t in Eq. 7. In practice, we select the larger one between those two estimations to optimize the compression ratio. For a small variable

Table 2: Point-wise QoI (x^2) error thresholds from different multivariate QoI function F and variable numbers ($c = 2$, $\beta = 0.9999$). Error threshold of $F(X)$ is T .

QoI	Variable Num. (n)	t from Theo. 5.3	t from Theo. 5.4
$x^2 + y^2 + z^2$	3	$0.33T$	$0.26T$
$\frac{1}{n} \sum x^2$	2^3	T	$1.27T$
	4^3	T	$3.6T$

number n , Theorem 5.3 can often provide better estimations, and vice versa. Table 2 shows a few examples of the point-wise QoI (x^2) error tolerances deduced from Theorem 5.3 and 5.4. As the number of variables increases, Theorem 5.4 provides more aggressive estimations, and for limited variable numbers, Theorem 5.3 can provide better estimations. Although Theorem 5.4 is probabilistic and cannot guarantee a deterministic bound of the multivariate QoI error, the QoI validation module in the QPET will post-process the outlier data points so that the QoI error will still be strictly bounded in any case. Moreover, if we set a high confidence level (such as $\beta = 0.999$), the increase of t benefits the compression ratio much more than the overhead brought by correcting very few data points. Admittedly, Theorem 5.4 needs certain preliminary conditions of $\{D_i\}$, which are not always true. For example, a non-biased data error ϵ that satisfies $E(\epsilon) = 0$ may not lead to a close-to-zero $E(f(\epsilon))$, and the variance of compression errors is dependent on several other factors such as data characteristics and input error bound. Despite those, from Theorem 5.4, we can still get good enough estimations by selecting a conservative value of c .

5.2.2 Non-linear multivariate QoI. Beyond the linear format described in Eq. 5, regarding generalized multivariate QoI function $F(x_1, \dots, x_n)$, we use the linear approximation of it for computing point-wise error bounds, leveraging the first-order differentials of F . For each specific variable set $\{x_i\}$, we have:

$$F(x'_1, \dots, x'_n) \approx F(x_1, \dots, x_n) + \sum_i \frac{\partial F}{\partial x_i}(x_i)(x'_i - x_i) \quad (9)$$

Eq. 9 falls into the format of Eq. 5, with $C = F(x_1, \dots, x_n)$, $\alpha_i = \frac{\partial F}{\partial x_i}(x_i)$, and $f(x) = x - x_i$ (equivalent to $f(x) = x$). Therefore, we can use the Eq. 9 and Theorem 5.3/5.4 to determine the point-wise error bounds from F . It is worth noticing that, in this case, for different $\{x_i\}$, we will have different t from Theorem 5.3 and 5.4 as there are different α_i values from the partial derivatives.

In Algorithm 3, we combine the computation of point-wise data error bounds from multivariate QoI in either linear or non-linear format. When dealing with the linear format, the computation can often get simplified. For example, for linear multivariate QoIs, the t in Line 14 can be shared over data regions.

5.3 Optimizing Global Error Bound

So far, for the QoI-preserving compression task, we have calculated the point-wise error bound for each data point x_i , acquiring a set of error bounds $\{\epsilon_i\}$. The compression framework will quantize those error bounds and store the encoded quantized results in the compressed data. QPET leverages the same method as [19] to store the error bounds, and [19] showed that the storage overhead of those error bounds would substantially affect the compression ratio. Therefore, minimizing the compressed size of $\{\epsilon_i\}$ is essential

Algorithm 3 POINT-WISE ERROR BOUND ESTIMATION WITH MULTIVARIATE QOI CONSTRAINT

Input: input data $X = \{x_i\}$, Data regions $\mathcal{R} = \{R_i\}$ ($R_i = \{r_{ij}\}$, $id(r_{ij})$ is the global index of r_{ij} so $r_{ij} = x_{id(r_{ij})}$), global error bound ϵ_g , multivariate QoI function F , QoI error threshold T , estimation parameter c , and confidence level β .
Output: Point-wise data error bounds $\{\epsilon_i\}$ For multivariate QoI error constraint.

```

1: for  $i = 1 \rightarrow |X|$  do
2:    $\epsilon_i \leftarrow \epsilon_g$  /*Initialize all  $\epsilon_i$  with global error bound*/
3: end for
4: for  $R_i \in \mathcal{R}$  do /*Iterate through regions*/
5:   if  $F(R_i) = C + \sum_j a_j g(r_{ij})$  then /*Linear Format*/
6:      $f \leftarrow g$ 
7:      $\{\alpha_j\} \leftarrow \{a_j\}$ 
8:   else /*Non-linear*/
9:      $f \leftarrow f(x) = x$ 
10:     $\{\alpha_j\} \leftarrow \left\{ \frac{\partial F}{\partial x_j}(r_{ij}) \right\}$ 
11:   end if
12:    $t_1 \leftarrow \frac{T}{\sum_i |\alpha_i|}$  /*Theorem 5.3*/
13:    $t_2 \leftarrow cT \sqrt{\frac{1}{2 \sum_j \alpha_j^2 \ln \frac{2}{1-\beta}}}$  /*Theorem 5.4*/
14:    $t \leftarrow \max(t_1, t_2)$ 
15:   for  $r_{ij} \in R_i$  do /*Iterate through data value in regions*/
16:      $\epsilon \leftarrow \text{Compute\_cb\_univar}(r_{ij}, t, f, \epsilon)$  /*By Algorithm 2*/
17:      $\epsilon_{id(r_{ij})} \leftarrow \min(\epsilon_{id(r_{ij})}, \epsilon)$  /*update  $\epsilon_{id(r_{ij})}$ */
18:   end for
19: end for
20: return  $\{\epsilon_i\}$ 

```

in optimizing the overall compression ratio. Previously we have known that for each data point x_i , its corresponding error bound ϵ_i will be $\min(\epsilon_g, \epsilon_i^j)$, in which ϵ_g is the global data error bound and ϵ_i^j is the error bound computed from QoI error threshold. To this end, we need to determine ϵ_g from 2 aspects: ϵ_g should be relatively small so that for most data points, ϵ_i will equal ϵ_g and free from point-wise error-bound storage. Meanwhile, ϵ_g cannot be too small. Otherwise, the data compression ratio will be too low.

To this end, we proposed a two-step dynamic global error-bound auto-tuning strategy in QPET. After acquiring the set of point-wise error bounds $\{\epsilon_i\}$, in the first step, a set of quantiles (20%, 10%, 5%, 2%, 1%, 0.5%, 0.25%) is drawn from it as global error bound candidates, and then QPET identify the best from them in a sample-and-tests scheme described in [33]. In the second step, QPET further reduces ϵ_g over the distribution of $\{\epsilon_i\}$ until a steep decrease is detected. According to our preliminary experiments, saving fewer error-bound values is often more beneficial in improving the compression ratio than applying a slightly larger global error bound.

The details of the described strategy are featured in Algorithm 4. In Lines 1 to 7, QPET optimizes the global error bound by tests on sampled data. In Line 13, QPET checks whether the current error bound ϵ is still over a gentle linear slope between the initial ϵ_0 and a termination value ϵ_t (e.g., $\epsilon_t = 0.95\epsilon_0$), and stop the decreasing of ϵ_g if it will beneath that slope. The K thSmallest() operations in Algorithm 4 can be implemented by fast-selection and only need to be performed on reduced ranges of $\{\epsilon_i\}$. Therefore, all the operations in Algorithm 4 can be efficiently done with $\mathcal{O}(n + qn \log qn)$ time complexity in average, in which q is the quantile of ϵ_0 . In practice, QPET skips the second part of tuning (from Line 8) when q is larger than a threshold (0.005) to guarantee efficiency, bringing negligible overhead to the overall compression pipeline.

Algorithm 4 GLOBAL ERROR BOUND AUTO-TUNING

Input: point-wise data error bounds $\{\epsilon_i\}$ with size n , a dropping threshold coefficient $c_0 \leq 1$
Output: Auto-tuned global error bound ϵ_g

- 1: $E_c \leftarrow \{\}$
- 2: **for** $q \in \{0.2, 0.1, 0.05, 0.02, 0.01, 0.005, 0.0025\}$ **do**
- 3: $k \leftarrow \lfloor qn \rfloor$
- 4: $\epsilon \leftarrow \text{KthSmallest}(\{\epsilon_i\}, k)$ /* ϵ is the k^{th} -smallest of $\{\epsilon_i\}$ */
- 5: $E_c.\text{insert}((\epsilon, k))$
- 6: **end for**
- 7: $\epsilon_0, k_0 \leftarrow \text{cmpTest_BestCR}(E_c)$ /* ϵ_g achieves the best compression ratio in compression tests among all error bounds in E_c , save its current value in ϵ_0 */
- 8: $\epsilon_g \leftarrow \epsilon_0$
- 9: $E_p \leftarrow \text{partialSort}(\{\epsilon_i\}, k_0)$ /* E_p is the sorted k smallest values in $\{\epsilon_i\}$ */
- 10: $k \leftarrow k_0 - 1$ /*Start checking smaller error bounds*/
- 11: **while** $k \geq 0$ /*we regard minimum as 0th-smallest*/ **do**
- 12: $\epsilon \leftarrow E_p[k]$
- 13: **if** $\epsilon \geq (c_0 + \frac{k}{k_0}(1 - c_0))\epsilon_0$ /* ϵ is above a slope*/ **then**
- 14: $\epsilon_g \leftarrow \epsilon$ /*Update ϵ_g */
- 15: **else**
- 16: **break** /*Stop decreasing ϵ_g */
- 17: **end if**
- 18: $k \leftarrow k - 1$
- 19: **end while**
- 20: **return** ϵ_g

6 EVALUATIONS

We evaluate QPET using six real-world datasets and diverse QoIs. In particular, we integrate QPET into three top-performing compressors (SZ3 [29], HPEZ [35], and SPERR [24]) and compare them with the base compressors in terms of QoI preservation. We also compare with QoI-SZ [19], which is the only compressor that preserves certain families of symbolic QoIs. We omit comparison with MGARD [5] because it cannot preserve non-linear QoIs.

6.1 Experimental Setup

6.1.1 Experimental environment and datasets. we perform the evaluations on 6 real-world scientific datasets from diverse domains (details in Table 3). Experiments are operated on Purdue Anvil computing cluster [38] (each node is equipped with two 64-core AMD EPYC 7763 CPUs and 512GB DDR4 memory).

Table 3: Information of the datasets in experiments

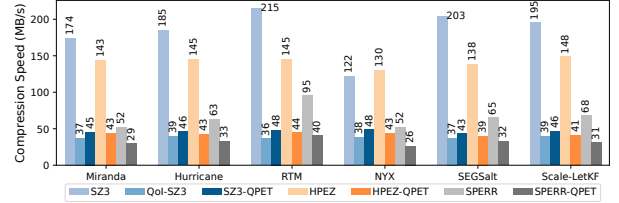
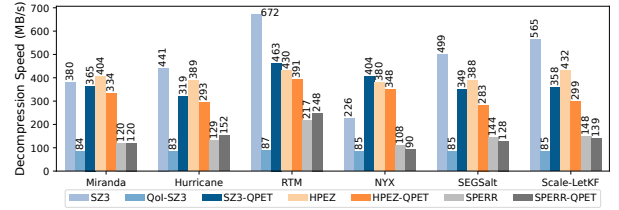
App.	# fields	Dimensions	Total Size	Domain
Miranda	7	256×384×384	1GB	Turbulence
Hurricane	13	100×500×500	1.3GB	Weather
RTM	11	449×449×235	2.0GB	Seismic Wave
NYX	6	512×512×512	3.1GB	Cosmology
SEGSalt	3	1008×1008×352	4.2GB	Geology
SCALE-LetKF	13	98×1200×1200	6.4GB	Climate

6.1.2 QoI functions, experimental configurations, and evaluation metrics. Table 4 shows the QoI functions to be preserved in the evaluation tasks. Among them, there are three different categories: point-wise, regional, and vector. They have diverse mathematical formats, and for many among them (such as e^x , $\frac{1}{x+c}$, and vector QoIs), QPET is the first framework that supports compression with preservation of those QoIs. The selection of QoI functions in our evaluation is based on existing investigations and analysis [19, 39, 50] of QoIs in practical scientific data analysis tasks.

In the tasks of QoI-preserving error-bounded lossy compression, Both a data error bound and a QoI error threshold are required. For the QPET-integrated compressors and QoI-SZ3, those threshold values are just input parameters. For base compressors, we use binary

Table 4: QoI functions in the evaluation

QoI type	QoI function	QoI type	QoI function
Pointwise	x^2	Regional	x^2 (average)
	$\log_2 x$		x^3 (average)
	e^x	Vector	$x^2 + y^2 + z^2$
	$\frac{1}{x+c}$		$\sqrt{x^2 + y^2 + z^2}$
	x^3		xyz

**Figure 3: Compression speed, $Q(x) = x^2$, $\tau = 1e-3$** **Figure 4: Decompression speed, $Q(x) = x^2$, $\tau = 1e-3$**

search to acquire the corresponding error-bounded to achieve the target QoI error threshold. Regarding the non-QPET compression configurations, we apply the optimization level of 3 (having close compression ratios to max level 4 and exhibiting better speed) and compression-ratio-preferred mode for HPEZ ($-T CR$) and the default setting for other configurations. Regarding QPET parameters in Algorithms 3, we set $c = 3$, $\beta = 0.999$ for SPERR, $c = 2$, $\beta = 0.999$ for HPEZ, and $c = 2$, $\beta = 0.99999$ for SZ3.

In evaluating the compression performance, the following widely-adopted metrics [19, 42] are used: (1) Compression and decompression speeds. (2) Compression ratio $CR = \frac{|X|}{|C|}$, which is the input data size $|X|$ divided by the data size $|C|$; (3) Bit rate $BR = \frac{|C| * 8 * \text{sizeof}(x)}{|X|}$, which is the number of bits in compressed data to store each value in the input. (3) Maximum data error and QoI error between the input and output; (4) PSNR [42] of the decompressed data QoI. The PSNR of QoI is define as $PSNR_Q = 20 \log_{10} \text{VRange}(Q(X)) - 10 \log_{10} \text{MSE}(Q(X), Q(X'))$, in which X and X' are the input/decompressed data, Q is the QoI function, VRange is value range, and MSE is mean squared error. The lower mean squared error between $Q(X)$ and $Q(X')$ lead to higher (better) PSNR. (5) Visualization of the QoI error between the original and decompressed data.

6.2 Evaluation Results

Here, we propose our solid evaluation results for QPET, which prove its advantages and versatility. Due to page limits, we selected the most representative results to be presented in this paper¹.

¹More evaluation results are available at our artifact link: <https://github.com/JLiu-1/QPET-Artifact>

Table 5: Showcase of QoI-preserving error-bounded lossy compression. non-QoI compressors are manually tuned with multi-runs. ϵ : data error bound. τ : QoI error threshold. CR: Compression ratio. $\max e_d$: maximum data error. $\max e_q$: maximum QoI error. All error values are relative (absolute value divided by value range).

QoI			$Q(x) = x^2$						$Q(x, y, z) = \sqrt{x^2 + y^2 + z^2}$					
Data field			SegSalt-Pressure2000			RTM-3500			hurricane-(u, v, w)			miranda-(v_x, v_y, v_z)		
ϵ	τ	Compressor	CR	$\max e_d$	$\max e_t$	CR	$\max e_d$	$\max e_t$	CR	$\max e_d$	$\max e_t$	CR	$\max e_d$	$\max e_t$
1E-2	1E-3	SZ3	75.8	2.7E-4	9.8E-4	25.3	2.7E-4	9.8E-4	17.5	4.2E-4	9.8E-4	124	5.6E-4	9.6E-4
		HPEZ	107	2.9E-4	1.0E-3	26.4	2.7E-4	9.8E-4	19.2	4.2E-4	9.7E-4	180	5.9E-4	1.0E-3
		SPERR	109	3.0E-4	9.7E-4	34.7	2.8E-4	9.5E-4	27.7	4.3E-4	1.0E-3	172.8	6.3E-4	1.0E-3
		QoI-SZ3	169	2.0E-3	1.0E-3	64.2	1.0E-3	1.0E-3	N/A	N/A	N/A	N/A	N/A	N/A
		SZ3-QPET	181	3.5E-3	1.0E-3	78.9	1.5E-3	1.0E-3	21.3	2.1E-3	1.0E-3	163	1.2E-3	9.7E-4
		HPEZ-QPET	195	3.5E-3	1.0E-3	94.1	1.5E-3	1.0E-3	22.8	2.1E-3	1.0E-3	227	1.2E-3	9.7E-4
		SPERR-QPET	182	2.7E-3	1.0E-3	66	4.6E-3	1.0E-3	34.9	2.4E-3	1.0E-3	202	1.2E-3	8.4E-4
1E-3	1E-4	SZ3	26.3	2.7E-5	9.5E-5	7.9	2.7E-5	9.5E-5	7.6	4.1E-5	9.7E-5	36.8	5.8E-5	9.9E-5
		HPEZ	31.7	2.7E-5	1.0E-4	8.3	2.8E-5	1.0E-4	7	4.1E-5	9.7E-5	46.8	5.8E-5	9.9E-5
		SPERR	44.2	3.1E-5	1.0E-4	9.1	2.9E-5	9.6E-5	9.9	4.1E-5	9.6E-5	58.6	5.9E-5	9.6E-5
		QoI-SZ3	70.2	8.0E-4	1.0E-4	18.7	2.0E-4	1.0E-4	N/A	N/A	N/A	N/A	N/A	N/A
		SZ3-QPET	72.1	9.4E-4	1.0E-4	19.3	2.2E-4	1.0E-4	7.5	2.1E-4	1.0E-4	43.7	1.2E-4	9.8E-5
		HPEZ-QPET	72.7	9.4E-4	1.0E-4	19.3	2.2E-4	1.0E-4	8	2.1E-4	1.0E-4	54.4	1.2E-4	9.8E-5
		SPERR-QPET	73.4	2.8E-4	1.0E-4	15.3	4.9E-4	1.0E-4	12.2	2.4E-4	1.0E-4	67.4	1.2E-4	8.9E-5
QoI			$Q(x) = \log_2 x$											
Data field			NYX-Baryon Density			NYX-Temperature			Scale-LetKF-PRES			Scale-LetKF-T		
ϵ	τ	Compressor	CR	$\max e_d$	$\max e_t$	CR	$\max e_d$	$\max e_t$	CR	$\max e_d$	$\max e_t$	CR	$\max e_d$	$\max e_t$
1E-1	1E-2	SZ3	15.1	8.0E-8	9.9E-3	30.2	3.7E-5	9.8E-3	322	8.8E-4	9.7E-3	982	7.4E-3	9.6E-3
		HPEZ	15.2	7.6E-8	9.9E-3	32.9	3.7E-5	9.9E-3	730	9.3E-4	9.8E-3	775	7.8E-3	1.0E-2
		SPERR	19.4	1.2E-7	9.7E-3	38.7	5.0E-5	9.8E-3	3744	9.4E-3	9.5E-3	1219	8.4E-3	9.7E-3
		QoI-SZ3	16.5	3.5E-7	1.0E-2	36.9	6.9E-5	1.0E-2	1197	1.3E-2	1.0E-2	717.3	5.4E-3	1.0E-2
		SZ3-QPET	28.1	2.2E-7	1.0E-2	39.7	5.3E-5	1.0E-2	435	2.8E-3	1.0E-2	1364	7.5E-3	9.8E-3
		HPEZ-QPET	27.9	2.2E-7	1.0E-2	42.9	5.3E-5	1.0E-2	421	2.8E-3	1.0E-2	758	7.5E-3	9.6E-3
		SPERR-QPET	35.6	3.4E-7	1.0E-2	55.7	8.3E-5	1.0E-2	1677	1.4E-3	4.6E-3	1401	8.8E-3	8.9E-3
1E-2	1E-3	SZ3	5.9	8.1E-9	9.8E-4	8.4	4.0E-6	9.8E-4	58	8.8E-5	1.0E-3	73	7.4E-4	9.8E-4
		HPEZ	6.2	7.6E-9	9.6E-4	9.1	3.7E-6	9.9E-4	61	8.5E-5	9.7E-4	104	7.4E-4	9.8E-4
		SPERR	6.3	7.4E-9	9.6E-4	8.8	3.7E-6	9.9E-4	188	9.8E-5	9.8E-4	146	7.8E-4	9.9E-4
		QoI-SZ3	7.3	3.5E-8	1.0E-3	9.4	6.9E-5	1.0E-3	280.6	2.6E-3	1.0E-3	67.9	9.6E-4	1.0E-3
		SZ3-QPET	8.8	3.6E-8	1.0E-3	10.8	6.8E-6	1.0E-3	71.6	2.9E-4	1.0E-3	88.2	7.5E-4	9.9E-4
		HPEZ-QPET	9.2	3.6E-8	1.0E-3	11.1	6.8E-6	1.0E-3	126	2.9E-4	1.0E-3	105	7.5E-4	9.8E-4
		SPERR-QPET	9.2	3.6E-8	1.0E-3	11.4	8.5E-6	1.0E-3	327	2.8E-4	1.0E-3	168	8.8E-4	1.0E-3

6.2.1 Competitive speeds. First, we measure and profile the execution speeds of QPET-integrated error-bounded lossy compressors to examine how much overhead QPET has introduced into those compressors. From the compression and decompression speeds on the Anvil cluster with the QoI function $Q(x) = x^2$ and the relative QoI error threshold $\tau = 1e-3$, reported in Figure 3 and 4, we can conclude as follows: QPET-integrated compressors keep reasonable and acceptable compression throughputs (20% ~ 30% of original SZ3/HPEZ and 40% ~ 60% of original SPERR), and the speed degradation is reasonable because it mainly lie in the determination of best-fit data error bounds. Without similar techniques, traditional compressors need to perform repeated executions to figure out an adequate global data error bound for acquiring a certain QoI error threshold. Our preliminary evaluations suggest this task may cost 10 or even more compression executions and QoI validations. More importantly, QPET brings quite limited time overheads in the decompression process (because neither error-bound computation nor QoI validation is needed), and sometimes it even improves the decompression speed over traditional compressors due to the reduced accuracy required in the compression to ensure the same QoI error threshold. Compared to the existing QoI-SZ3, for the same use cases, QPET gains 20% ~ 30% compression speed improvement and up to 400% decompression speed improvement, which is exciting.

6.2.2 Representative showcases. For the tasks of QoI-preserving data compression on 8 different data snapshots with 3 sets of error-bound parameters and 3 QoI functions, in Table 5, we present

several metrics of the compression results from different error-bounded lossy compressors, including the compression ratio and maximum data/QoI errors (no results for QoI-SZ3 on $Q(x, y, z) = \sqrt{x^2 + y^2 + z^2}$ because it doesn't support vector QoIs). The results from non-QoI-integrated compressors are acquired by manual tuning described in Section 6.1.2, and each result entry from QoI-integrated compressors is from a single run. Table 5 indicates multiple key findings: (1) QPET-integrated compressors have strictly bounded both the data error and QoI error under different parameter sets ($\epsilon = 1e-1$ & $\tau = 1e-2$, $\epsilon = 1e-2$ & $\tau = 1e-3$, and $\epsilon = 1e-3$ & $\tau = 1e-4$), ensuring $\max e_d \leq \epsilon$ and $\max e_q \leq \tau$; (2) Under the same error thresholds, each QPET-integrated compressor achieved much higher compression ratios than the base compressor. For example, on RTM data snapshot #3500, with $Q(x) = x^2$, $\epsilon = 1e-2$ and $\tau = 1e-3$, HPEZ-QPET's compression ratio (94.1) is 256% higher than HPEZ. Moreover, featuring the same base compression pipeline, SZ3-QPET consistently gained better compression ratios than QoI-SZ3, exhibiting the advantage of QPET over the QoI-preservation module in QoI-SZ3. On the Baryon Density field of the NYX dataset, with $Q(x) = \log_2 x$, $\epsilon = 1e-1$ and $\tau = 1e-2$, SZ3-QPET's compression ratio is 1.7 \times of SZ3-QoI. (3) To meet the same QoI error threshold, non-QoI-integrated compressors usually over-preserve per-data quality, exhibiting much lower maximum data error than QoI-integrated compressors. This explains why non-QoI-integrated compressors have limited compression ratios on QoI-preserving compression tasks and proves the effectiveness of controlling data error with point-wise precisions.

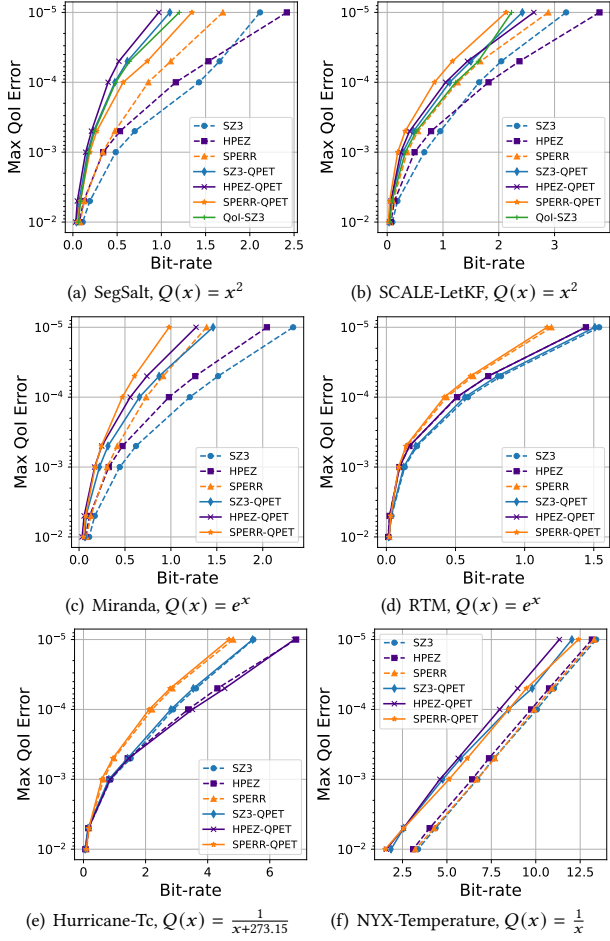


Figure 5: Bit rate and max QoI error plots (point-wise QoIs).

6.2.3 Improved Compression Ratios. To comprehensively understand the compression ratio improvement brought by QPET in the QoI-preserving error-bounded data compression, the compressors mentioned above are evaluated on a large variety of QoI functions and error thresholds. Then, we plot the bit rates (reciprocal of compression ratio) and maximum QoI errors (relative, divided by value range), showing that QPET-integrated compressors have substantially improved the compression ratio (bit rate) when achieving the same maximum QoI errors as others. Due to the page limit, we will show the most representative results among plenty of excellent outcomes we acquired in diverse test cases.

Regarding 3 different point-wise QoI functions, Figure 5 presents the bit rate-maximum QoI error plots we acquired on 6 data domains. In this figure and all other similar ones in the paper, for better visibility of comparison, the results from the same base compressors are plotted in the curves of the same color, with QPET-integrated ones solid and non-QPET ones dashed. Moreover, the results from QoI-SZ3 appear if and only if the QoI is supported by QoI-SZ3 (i.e., the QoIs fall into the four families in [19]). In Figure 5, integrating QPET into the compressors has shown improvements or at least the same bit rates (so the same CR as well) when the QoI error threshold is fixed. For example, on the Scale-LetKF dataset, QPET-integrated

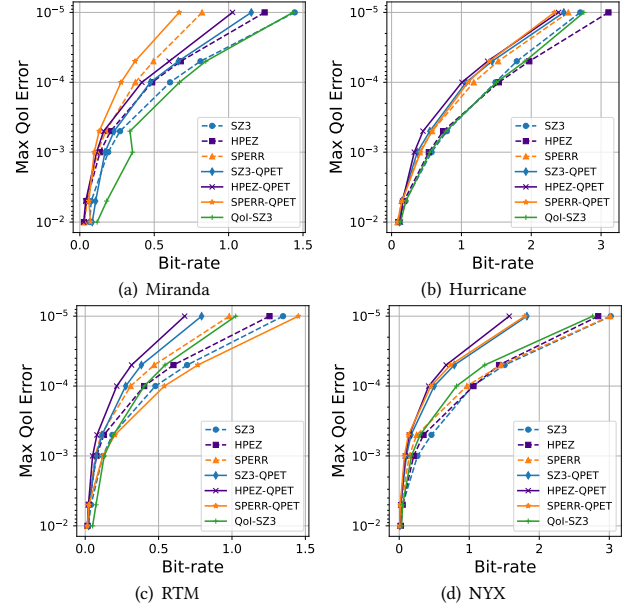


Figure 6: Bit rate and max QoI error plots of compressors ($Q(X) = \frac{1}{n_b} \sum x^2$, $n_b = 4^3$, i.e. average x^2 on $4 \times 4 \times 4$ blocks).

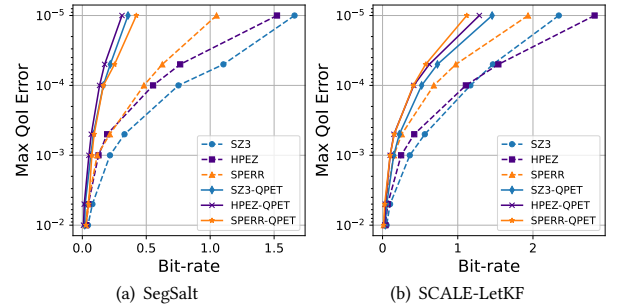


Figure 7: BR-max QoI error plots ($Q(X) = \frac{1}{n_b} \sum x^3$, $n_b = 4^3$).

SZ3 can achieve $\sim 140\%$ compression ratio improvement over SZ3 when the error threshold for the square of data ($Q(x) = x^2$) is set as $1e-3$ of the whole square value range. In the same case, compared to QoI-SZ3, QPET-SZ3 also gains 16%/20% CR improvement when the square QoI error threshold is $1e-3/1e-4$. QPET also benefits more compressors than SZ3, bringing 88% CR improvement to prediction-based HPEZ when compressing the Miranda dataset with a QoI $Q(x) = e^x$ tolerance of relatively $1e-3$, and 10% CR improvement to transform-based SPERR when compressing the Hurricane Tc data field with a QoI $Q(x) = \frac{1}{x+273.15}$ tolerance of relatively $1e-4$. Admittedly, QPET does not always improve the compression ratio over the base compressors. However, QPET can always bring no worse compression ratios, and as discussed in Section 6.2.1, non-QoI compressors need many complete compression executions in the trial-and-validation of QoI errors to achieve the compression ratio reported. Therefore, QPET constantly improves either the compression ratio or the time cost for the QoI-preserving compression tasks (in many cases, it can do both).

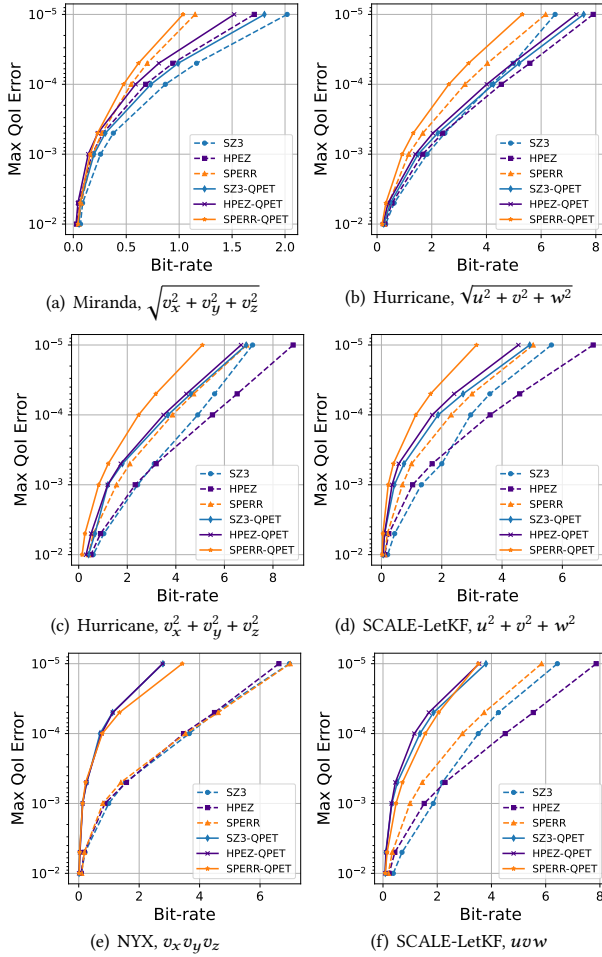


Figure 8: Bit rate and max QoI error plots (vector QoIs).

For multivariate QoI functions, we evaluated two sub-types: QoI on data blocks within one data field and QoI vector data among multiple fields. In Figure 6, we evaluate QPET and the baselines on a fundamental blockwise QoI function: the average of x^2 on partitioned fixed-size data blocks. We selected this QoI for evaluation because QoI-SZ3 also supports it, so we can directly compare our work to it in this benchmark. Comparing the results from SZ3-QPET and QoI-SZ3 in Figure 6, it is clear that the QPET has significantly outperformed QoI-SZ3 (which showed unstable performance) in terms of compression ratio. On the Miranda dataset, SZ3-QPET’s compressor ratio is 75% higher than QoI-SZ3 when $\tau = 1e-3$. When compared to manually-tuned base compressors, SPERR-QPET gains 116% CR improvement over SPERR on the NYX dataset under $\tau = 1e-4$. The improvement of compression ratios in these test cases is attributed to Theorem 5.4 because of the large variable numbers (as the block size 64) so that we can apply much higher point-wise QoI (x^2) error thresholds on each data point compared to the overall error threshold.

In Figure 7 and 8, we also evaluate several other multivariate QoIs on QPET, which are unsupported by other existing works. Figure 7 presents the QoI-preserved compression on block average

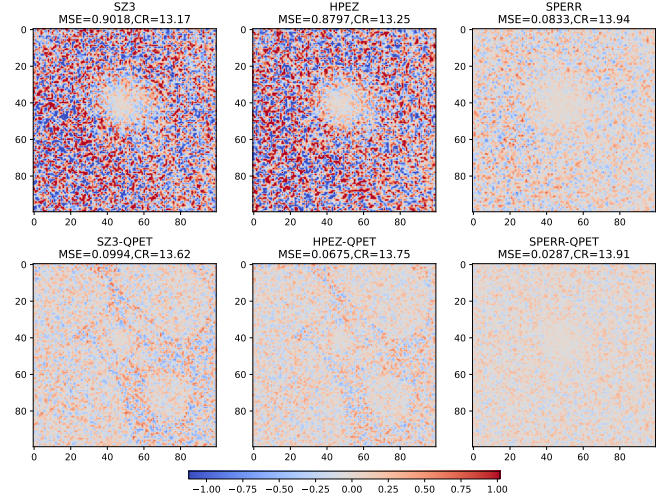


Figure 9: Error visualization of $u^2 + v^2 + w^2$ of Hurricane. The slice is $[6, 100:200, 100:200]$.

of x^3 . Similarly with the average x^2 SZ3/HPEZ-QPET achieved incredible compression ratio improvements over SZ3/HPEZ. Besides, we evaluated 3 vector QoIs, on all the 3D velocity vectors (across 3 data snapshots) in those datasets. Over vector QoIs, QPET provides satisfactory compression ratio improvements under all test cases. For the hurricane dataset, with $Q(x) = \sqrt{u^2 + v^2 + w^2}$ and $\tau = 1e-3$, QPET on SPERR improve the compression ratio by 25%. For the Hurricane dataset, with $Q(x) = u^2 + v^2 + w^2$ and $\tau = 1e-4$, QPET on all compressors improves the CR by more than 30%.

Last, we noticed that in one case (Figure 6 (c)), SPERR-QPET delivered worse compression ratios than SPERR. This is because the current data sampling strategy in the global error-bounded tuning implementation of QPET-SPRR is sub-optimal in a few cases. We will resolve this issue in the next update by leveraging the data sampling strategy in [34].

6.2.4 Well-preserved QoI quality. Beyond the maximum QoI error, QPET also preserves or refines the overall decompression QoI quality well. Figure 10 presents 6 Bit rate and the QoI-PSNR plots on 6 datasets and 6 QoIs. Due to the intrinsic of SPERR (no point-wise error bound), integrating QPET into it doesn’t significantly improve the PSNR, but it is also never degraded, and SZ3/HPEZ-QPET can acquire improved PSNR over SZ3/HPEZ, which proves the importance of applying different point-wise error bounds on data values. On the SegSalt dataset ($Q(x) = x^3$), SZ3-QPET achieves a 102% CR improvement over SZ3 when the decompressed QoI PSNR is 90. On the velocity fields of Hurricane ($Q(u, v, w) = \sqrt{u^2 + v^2 + w^2}$), SPERR-QPET achieves a 23% CR improvement over SPERR when the decompressed QoI PSNR is 92.

Additionally, we visualize some decompressed QoI errors on the velocity of the Hurricane datasets. In Figure 9, on a 2D slice of decompression results aligned with $CR \approx 13$, the QPET-integrated compressors all gained much better QoI Mean-square Error and reduced error patterns compared to the baselines.

6.2.5 Ablation study. At the end of our evaluation, we commit an ablation study of QPET design components, separately validating

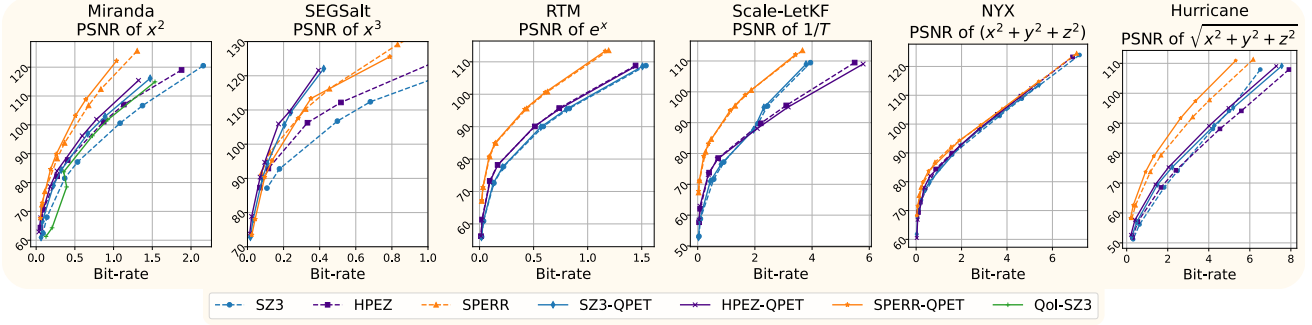


Figure 10: Bit-Rate and QoI PSNR plots in QoI-preserving error-bounded lossy compression.

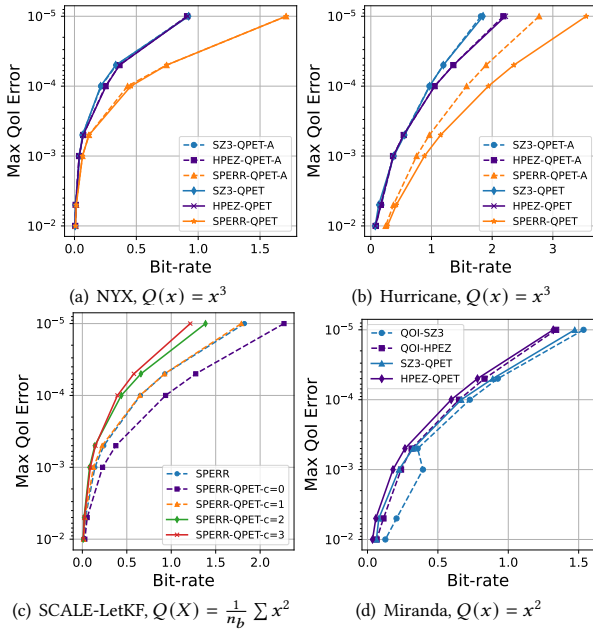


Figure 11: Ablation study on QPET Components.

how different strategies described in Algorithm 2, 3, and 4 contribute to the performance of QPET.

On bounding the error of $Q(x) = x^3$, Figure 11 (a) and (b) compare QPET to its derivation QPET-A, which uses the analytical solution of inequality $|(\epsilon_i + x_i)^3 - x_i^3| \leq \tau$ instead of Algorithm 2 to determine the point-wise error bound ϵ_0 for x_0 . On the Nyx dataset, QPET achieves the same compression ratio as QPET-A (almost overlapped curves of QPET and QPET-A), meaning that Algorithm 2 performed well to replace analytic solutions. On the hurricane dataset, QPET also did good jobs for SZ3/HPEZ, but SPERR-QPET-A provides better CR than SPERR-QPET, indicating that Algorithm 2 is not optimized for SPERR. The reasons are two-fold: (1) Hurricane datasets contain several close-to-zero data fields, for which Algorithm 2 is inaccurate with $Q(x) = x^3$; (2) SPERR doesn't support point-wise data encoding accuracy, which explains the divergent performances between SZ3/HPEZ-QPET and SPERR-QPET. In future works, we would like to customize the implementation of SPERR-QPET to support point-wise data accuracy.

Next, we investigate the impact of Thorem 5.4 and the parameter c by evaluating SPERR-QPET on the SCALE-LetKF with the QoI of the average of x^2 on $4 \times 4 \times 4$ data blocks with different configurations. Under $c = 0$, SPERR-QPET deactivates Theorem 5.4, and larger c brings large error bound estimations from Thorem 5.4. Figure 11 (c) illustrates the corresponding results. Higher c does improve compression by proposing higher and still trustworthy estimations of point-wise error bounds. As the improvement of compression ratios becomes minor when c arrives at 3.0, we selected this value as the default in SPERR-QPET.

Last, in Figure 11 (d), we verify the stability and quality of QPET's global error-bound tuning mechanism (Algorithm 4). To this end, with $Q(x) = x^2$, we compared SZ3/HPEZ-QPET to QoI-SZ3/HPEZ (QoI-HPEZ leverages the QoI-SZ3-style global error selection on HPEZ-QPET). On the Miranda dataset, SZ3-QPET resolves the instability of QoI-SZ3, and HPEZ-QPET provides better compression ratios (5% ~ 20% across different QoI error thresholds) than QoI-HPEZ. According to these results and more similar ones we acquired, we can state that Algorithm 4 achieves state-of-the-art for global error-bound tuning.

7 CONCLUSION

In this work, we propose QPET, a versatile and portable framework for error-bounded lossy compression that enables the preservation of a broad range of Quantity-of-Interest (QoI) while significantly improving the performance and quality of existing QoI-preserving error-bounded lossy compression. We further integrate QPET into 3 state-of-the-art error-bounded lossy compressors of different archetypes. Experimental results demonstrate that QPET is faster than the existing QoI-preserving error-bounded lossy compression framework and leads to up to 250% compression ratio improvements over the base compressors while eliminating the iterative tuning procedure. QPET also delivers up to 75% compression ratio improvements over existing QoI-preserving lossy compressors. In future research, we will optimize QPET in the following three aspects: (1) Improve the inclusivity of QPET to enable the support for more error-bounded lossy compression pipelines and real-world QoI formats; (2) Investigate more stable and optimized strategies for optimizing the point-wise and global error bounds for optimizing the compression ratio and data quality; (3) Enhance the throughput of QPET to reduce the computational cost for QoI preservation in the error-bounded lossy compression tasks.

REFERENCES

- [1] [n.d.]. nvCOMP. <https://github.com/NVIDIA/nvcomp>.
- [2] [n.d.]. SymEngine: A fast symbolic manipulation library. <https://github.com/symengine/symengine>.
- [3] 2021. Team at Princeton Plasma Physics Laboratory employs DOE supercomputers to understand heat-load width requirements of future ITER device. <https://www.olcf.ornl.gov/2021/02/18/scientists-use-supercomputers-to-study-reliable-fusion-reactor-design-operation>. Online.
- [4] Nitin Agrawal and Ashish Vulimiri. 2017. Low-latency analytics on colossal data streams with summarystore. In *Proceedings of the 26th Symposium on Operating Systems Principles*. 647–664.
- [5] Mark Ainsworth, Ozan Tugluk, Ben Whitney, and Scott Klasky. 2019. Multilevel techniques for compression and reduction of scientific data-quantitative control of accuracy in derived quantities. *SIAM Journal on Scientific Computing* 41, 4 (2019), A2146–A2171.
- [6] Jyrki Alakuijala, Andrea Farruggia, Paolo Ferragina, Eugene Kliuchnikov, Robert Obyrk, Zoltan Szabadka, and Lode Vandevenne. 2018. Brotli: A general-purpose data compressor. *ACM Transactions on Information Systems (TOIS)* 37, 1 (2018), 1–30.
- [7] Andrei Arion, Angela Bonifati, Ioana Manolescu, and Andrea Pugliese. 2007. XQueC: A query-conscious compressed XML database. *ACM Transactions on Internet Technology (TOIT)* 7, 2 (2007), 10–es.
- [8] Benjamin Bross, Ye-Kui Wang, Yan Ye, Shan Liu, Jianle Chen, Gary J Sullivan, and Jens-Rainer Ohm. 2021. Overview of the versatile video coding (VVC) standard and its applications. *IEEE Transactions on Circuits and Systems for Video Technology* 31, 10 (2021), 3736–3764.
- [9] Zhiyuan Chen, Johannes Gehrke, and Flip Korn. 2001. Query optimization in compressed database systems. In *Proceedings of the 2001 ACM SIGMOD international conference on Management of data*. 271–282.
- [10] Yann Collet. 2015. Zstandard – Real-time data compression algorithm. <http://facebook.github.io/zstd/> (2015).
- [11] L Peter Deutsch. 1996. GZIP file format specification version 4.3.
- [12] Hazem Elmelegy, Ahmed K. Elmagarmid, Emmanuel Cecchet, Walid G. Aref, and Willy Zwaenepoel. 2009. Online Piece-Wise Linear Approximation of Numerical Streams with Precision Guarantees. *Proc. VLDB Endow.* 2, 1 (Aug. 2009), 145–156.
- [13] Ian Foster, Mark Ainsworth, Bryce Allen, Julie Bessac, Franck Cappello, Jong Youl Choi, Emil Constantinescu, Philip E Davis, Sheng Di, Wendy Di, Hanqi Guo, Scott Klasky, Kerstin Kleese Van Dam, Tahsin Kurc, Qing Liu, Abid Malik, Kshitij Mehta, Klaus Mueller, Todd Munson, George Ostouchov, Manish Parashar, Tom Peterka, Line Pouchard, Dingwen Tao, Ozan Tugluk, Stefan Wild, Matthew Wolf, Justin M. Wozniak, Wei Xu, and Shinjae Yoo. 2017. Computing just what you need: Online data analysis and reduction at extreme scales. In *European conference on parallel processing*. Springer, 3–19.
- [14] Qian Gong, Xin Liang, Ben Whitney, Jong Youl Choi, Jieyang Chen, Lipeng Wan, Stéphane Ethier, Seung-Hoe Ku, R Michael Churchill, C-S Chang, et al. 2021. Maintaining trust in reduction: Preserving the accuracy of quantities of interest for lossy compression. In *Smoky Mountains Computational Sciences and Engineering Conference*. Springer, 22–39.
- [15] Qian Gong, Xin Liang, Ben Whitney, Jong Youl Choi, Jieyang Chen, Lipeng Wan, Stéphane Ethier, Seung-Hoe Ku, R Michael Churchill, C-S Chang, et al. 2021. Maintaining trust in reduction: Preserving the accuracy of quantities of interest for lossy compression. In *Smoky Mountains Computational Sciences and Engineering Conference*. Springer, 22–39.
- [16] Wassily Hoeffding. 1963. Probability Inequalities for Sums of Bounded Random Variables. *J. Amer. Statist. Assoc.* 58, 301 (1963), 13–30. <http://www.jstor.org/stable/2282952>
- [17] Lawrence Ibarria, Peter Lindstrom, Jarek Rossignac, and Andrzej Szymczak. 2003. Out-of-core compression and decompression of large n-dimensional scalar fields. In *Computer Graphics Forum*, Vol. 22. Wiley Online Library, 343–348.
- [18] Søren Kejser Jensen, Torben Bach Pedersen, and Christian Thomsen. 2018. Modelfdb: Modular model-based time series management with spark and cassandra. *Proceedings of the VLDB Endowment* 11, 11 (2018), 1688–1701.
- [19] Pu Jiao, Sheng Di, Hanqi Guo, Kai Zhao, Jiannan Tian, Dingwen Tao, Xin Liang, and Franck Cappello. 2022. Toward Quantity-of-Interest Preserving Lossy Compression for Scientific Data. *Proceedings of the VLDB Endowment* 16, 4 (2022), 697–710.
- [20] Søren Kejser Jensen, Torben Bach Pedersen, and Christian Thomsen. 2019. Scalable Model-Based Management of Correlated Dimensional Time Series in ModelDB+. *arXiv e-prints* (2019), arXiv–1903.
- [21] Fabian Knorr, Peter Thoman, and Thomas Fahringer. 2021. ndzip: A high-throughput parallel lossless compressor for scientific data. In *2021 Data Compression Conference (DCC)*. IEEE, 103–112.
- [22] Fabian Knorr, Peter Thoman, and Thomas Fahringer. 2021. ndzip-gpu: efficient lossless compression of scientific floating-point data on GPUs. In *Proceedings of the International Conference for High Performance Computing, Networking, Storage and Analysis*. 1–14.
- [23] I. Lazaridis and S. Mehrotra. 2003. Capturing sensor-generated time series with quality guarantees. In *Proceedings 19th International Conference on Data Engineering (Cat. No.03CH37405)*. 429–440. <https://doi.org/10.1109/ICDE.2003.1260811>
- [24] Shaomeng Li, Peter Lindstrom, and John Clyne. 2023. Lossy scientific data compression with SPERR. In *2023 IEEE International Parallel and Distributed Processing Symposium (IPDPS)*. IEEE, 1007–1017.
- [25] Panagiotis Liakos, Katia Papakonstantinou, and Yannis Kotidis. 2022. Chimp: efficient lossless floating point compression for time series databases. *Proceedings of the VLDB Endowment* 15, 11 (2022), 3058–3070.
- [26] Xin Liang, Sheng Di, Franck Cappello, Mukund Raj, Chunhui Liu, Kenji Ono, Zizhong Chen, Tom Peterka, and Hanqi Guo. 2022. Toward feature-preserving vector field compression. *IEEE Transactions on Visualization and Computer Graphics* 29, 12 (2022), 5434–5450.
- [27] Xin Liang, Sheng Di, Dingwen Tao, Sihuan Li, Shaomeng Li, Hanqi Guo, Zizhong Chen, and Franck Cappello. 2018. Error-Controlled Lossy Compression Optimized for High Compression Ratios of Scientific Datasets. In *2018 IEEE International Conference on Big Data*. IEEE.
- [28] Xin Liang, Hanqi Guo, Sheng Di, Franck Cappello, Mukund Raj, Chunhui Liu, Kenji Ono, Zizhong Chen, and Tom Peterka. 2020. Toward Feature-Preserving 2D and 3D Vector Field Compression. In *PacificVis*. 81–90.
- [29] Xin Liang, Kai Zhao, Sheng Di, Sihuan Li, Robert Underwood, Ali M. Gok, Jiannan Tian, Junjing Deng, Jon C. Calhoun, Dingwen Tao, Zizhong Chen, and Franck Cappello. 2023. SZ3: A Modular Framework for Composing Prediction-Based Error-Bounded Lossy Compressors. *IEEE Transactions on Big Data* 9, 2 (2023), 485–498. <https://doi.org/10.1109/TBDATA.2022.3201176>
- [30] Peter Lindstrom. 2014. Fixed-rate compressed floating-point arrays. *IEEE transactions on visualization and computer graphics* 20, 12 (2014), 2674–2683.
- [31] Peter G Lindstrom et al. 2017. *Fpzip*. Technical Report. Lawrence Livermore National Lab.(LLNL), Livermore, CA (United States).
- [32] Chunwei Liu, Hao Jiang, John Papparrizos, and Aaron J Elmore. 2021. Decomposed bounded floats for fast compression and queries. *Proceedings of the VLDB Endowment* 14, 11 (2021), 2586–2598.
- [33] Jinyang Liu, Sheng Di, Kai Zhao, Xin Liang, Zizhong Chen, and Franck Cappello. 2022. Dynamic quality metric oriented error bounded lossy compression for scientific datasets. In *2022 SC22: International Conference for High Performance Computing, Networking, Storage and Analysis (SC)*. IEEE Computer Society, 892–906.
- [34] Jinyang Liu, Sheng Di, Kai Zhao, Xin Liang, Zizhong Chen, and Franck Cappello. 2023. FAZ: A flexible auto-tuned modular error-bounded compression framework for scientific data. In *Proceedings of the 37th International Conference on Supercomputing*. 1–13.
- [35] Jinyang Liu, Sheng Di, Kai Zhao, Xin Liang, Sian Jin, Zizhe Jian, Jiajun Huang, Shixun Wu, Zizhong Chen, and Franck Cappello. 2024. High-performance effective scientific error-bounded lossy compression with auto-tuned multi-component interpolation. *Proceedings of the ACM on Management of Data* 2, 1 (2024), 1–27.
- [36] Kiyoshi Masui, Mandana Amiri, Liam Connor, Meiling Deng, Mateus Fandino, Carolin Höfer, Mark Halpern, David Hanna, Adam D Hincks, Gary Hinshaw, et al. 2015. A compression scheme for radio data in high performance computing. *Astronomy and Computing* 12 (2015), 181–190.
- [37] Tuomas Pelkonen et al. 2015. Gorilla: A Fast, Scalable, in-Memory Time Series Database. *Proc. VLDB Endow.* 8, 12 (Aug. 2015), 1816–1827.
- [38] X Carol Song, Preston Smith, Rajesh Kalyanam, Xiao Zhu, Eric Adams, Kevin Colby, Patrick Finnegan, Erik Gough, Elizabeth Hillery, Rick Irvine, et al. 2022. Anvil-system architecture and experiences from deployment and early user operations. In *Practice and experience in advanced research computing*. 1–9.
- [39] Zhaoyuan Su, Sheng Di, Ali Murat Gok, Yue Cheng, and Franck Cappello. 2022. Understanding impact of lossy compression on derivative-related metrics in scientific datasets. In *2022 IEEE/ACM 8th International Workshop on Data Analysis and Reduction for Big Scientific Data (DRBSD)*. IEEE, 44–53.
- [40] Vivienne Sze, Madhukar Budagavi, and Gary J Sullivan. 2014. High efficiency video coding (HEVC). In *Integrated circuit and systems, algorithms and architectures*. Vol. 39. Springer, 40.
- [41] Dingwen Tao, Sheng Di, Zizhong Chen, and Franck Cappello. 2017. Significantly improving lossy compression for scientific data sets based on multidimensional prediction and error-controlled quantization. In *2017 IEEE International Parallel and Distributed Processing Symposium*. IEEE, 1129–1139.
- [42] Dingwen Tao, Sheng Di, Hanqi Guo, Zizhong Chen, and Franck Cappello. 2019. Z-checker: A framework for assessing lossy compression of scientific data. *The International Journal of High Performance Computing Applications* 33, 2 (2019), 285–303. <https://doi.org/10.1177/1094342017737147>
- [43] David S Taubman and Michael W Marcellin. 2002. JPEG2000: Standard for interactive imaging. *Proc. IEEE* 90, 8 (2002), 1336–1357.
- [44] Jiannan Tian, Sheng Di, Xiaodong Yu, Cody Rivera, Kai Zhao, Sian Jin, Yunhe Feng, Xin Liang, Dingwen Tao, and Franck Cappello. 2021. cuSZ (x): Optimizing Error-Bounded Lossy Compression for Scientific Data on GPUs. *CoRR* (2021).

- [45] Jiannan Tian, Sheng Di, Kai Zhao, Cody Rivera, Megan Hickman Fulp, Robert Underwood, Sian Jin, Xin Liang, Jon Calhoun, Dingwen Tao, and Franck Cappello. 2020. cuSZ: An Efficient GPU-Based Error-Bounded Lossy Compression Framework for Scientific Data. In *Proceedings of the ACM International Conference on Parallel Architectures and Compilation Techniques* (Virtual Event, GA, USA) (PACT '20). Association for Computing Machinery, New York, NY, USA, 3–15. <https://doi.org/10.1145/3410463.3414624>
- [46] Roman Vershynin. 2018. *High-dimensional probability: An introduction with applications in data science*. Vol. 47. Cambridge university press.
- [47] Martin J Wainwright. 2019. *High-dimensional statistics: A non-asymptotic viewpoint*. Vol. 48. Cambridge university press.
- [48] Gregory K Wallace. 1991. The JPEG still picture compression standard. *Commun. ACM* 34, 4 (1991), 30–44.
- [49] Thomas Wiegand, Gary J Sullivan, Gisle Bjontegaard, and Ajay Luthra. 2003. Overview of the H. 264/AVC video coding standard. *IEEE Transactions on circuits and systems for video technology* 13, 7 (2003), 560–576.
- [50] Xuan Wu, Qian Gong, Jieyang Chen, Qing Liu, Norbert Podhorszki, Xin Liang, and Scott Klasky. 2024. Error-controlled Progressive Retrieval of Scientific Data under Derivable Quantities of Interest. In *2024 SC24: International Conference for High Performance Computing, Networking, Storage and Analysis SC*. IEEE Computer Society, 1368–1383.
- [51] Mingze Xia, Sheng Di, Franck Cappello, Pu Jiao, Kai Zhao, Jinyang Liu, Xuan Wu, Xin Liang, and Hanqi Guo. 2024. Preserving Topological Feature with Sign-of-Determinant Predicates in Lossy Compression: A Case Study of Vector Field Critical Points. In *2024 IEEE 40th International Conference on Data Engineering (ICDE)*. IEEE, 4979–4992.
- [52] Lin Yan, Xin Liang, Hanqi Guo, and Bei Wang. 2023. TopoSZ: Preserving topology in error-bounded lossy compression. *IEEE Transactions on Visualization and Computer Graphics* (2023).
- [53] Feng Zhang, Zaifeng Pan, Yanliang Zhou, Jidong Zhai, Xipeng Shen, Onur Mutlu, and Xiaoyong Du. 2021. G-TADOC: Enabling efficient GPU-based text analytics without decompression. In *2021 IEEE 37th International Conference on Data Engineering (ICDE)*. IEEE, 1679–1690.
- [54] Feng Zhang, Jidong Zhai, Xipeng Shen, Onur Mutlu, and Wenguang Chen. 2018. Efficient document analytics on compressed data: Method, challenges, algorithms, insights. *Proceedings of the VLDB Endowment* 11, 11 (2018), 1522–1535.
- [55] Kai Zhao, Sheng Di, Maxim Dmitriev, Thierry-Laurent D. Tonellot, Zizhong Chen, and Franck Cappello. 2021. Optimizing Error-Bounded Lossy Compression for Scientific Data by Dynamic Spline Interpolation. In *2021 IEEE 37th International Conference on Data Engineering (ICDE)*. 1643–1654. <https://doi.org/10.1109/ICDE51399.2021.00145>